

Energy-saving Potential Assessment of Building Energy System Considering Climate Impacts

Zhenwei Zhang, Hongxun Hui*

State Key Laboratory of Internet of Things for Smart City, University of Macau, Macao, 999078, China
Department of Electrical and Computer Engineering, University of Macau, Macao, 999078, China
Zhuhai UM Science Technology Research Institute, Zhuhai, 519031, China

Abstract—Photovoltaic/thermal integrated system (PV/T) and virtual energy storage system (VESS) are innovative and energy-saving techniques for multi-energy demand, providing building energy system (BES) with adjustable potential. However, due to inherent deviations in climate conditions, building demands and equipment performance, lack of confidence in energy-saving potential has been a tricky problem. To cope with that, an energy-saving potential assessment model considering climate conditions and user satisfaction is proposed in this paper. First, a typical BES model coupling PV/T and VESS is established. Meanwhile, we develop numerical relationships between varying climate conditions (solar radiation, temperature) and PV/T conversion efficiency, coefficient of performance (COP) for air conditioners, and storage capacity of VESS, respectively. Then, an optimal dispatch model with minimize electricity consumption is applied to assess the energy-saving potential, taking into account the user satisfaction. Simulation results on building block in University of Macau demonstrate the effectiveness of the proposed method and verify that 76% energy-saving potential can be achieved.

Index Terms—Photovoltaic/thermal integrated system, virtual energy storage system, building energy system, climate conditions.

I. INTRODUCTION

THE building sector consumes 36% of the world's energy and is responsible for 39% of global carbon emissions [1]. Under the goal of zero carbon emissions, more photovoltaics (PVs) are installed on building roofs and have become significant power resources [2]. Moreover, with the development of economy and society, air conditioners are increasing rapidly and become the largest power consumption loads in buildings [3]. Compared with traditional generators (e.g., thermal power plants) and loads (e.g., lights), both PVs and air conditioners can be easily impacted by the climate. Specifically, the varying climate conditions mainly bring two challenges:

- i) *In power supply side*: The real-time solar radiation can directly decide the power output of PVs [4], and the temperature can impact the generation efficiency of PV cells [5]. To improve the utilization efficiency of solar energy, photovoltaic/thermal integrated system (PV/T) has gained more attention. Compared with single PV generation, PV/T recovers waste heat from PV cells and combines heat pumps to meet the

This work is funded by the Science and Technology Development Fund, Macau SAR (File no. SKL-IOTSC(UM)-2021-2023, and File no. 0117/2022/A3). The corresponding author is Hongxun Hui (email: hongxunhui@um.edu.mo).

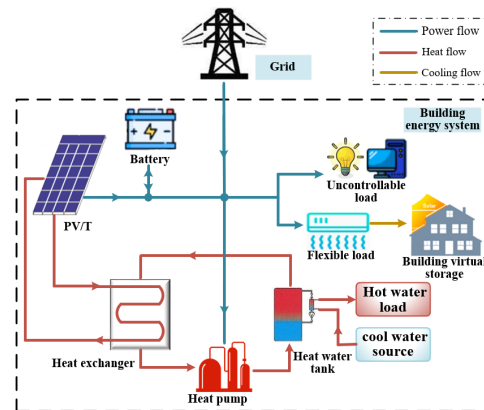


Fig. 1. Building energy system structure.

hot water demand of buildings [6]. A combined energy supply system consisting of 12 PV/T modules is evaluated in [7] to verify that the overall COP could reach 3.27. However, most studies are based on defined constant experimental parameters [8], which cannot accurately feature the operation characteristics under actual climate conditions.

- ii) *In power demand side*: The ambient temperature can extremely impact the cooling demand (e.g., the electricity consumption for air conditioners already exceeds 40% of the total load [9]). The refrigeration process of air conditioners includes compression, evaporation, expansion, and condensation, which can also be impacted by the ambient temperature. When the outside unit of the air conditioner is under a higher ambient temperature, the coefficient of performance (COP) will drop rapidly. Especially during the peak load period at noon, the drop of COP can further aggravate the power consumption.

To address the above issue, some studies are paying to energy storage systems, including the battery and virtual energy storage system (VESS) by utilizing building thermal inertia [10]. The VESS capacity of a building is determined by the climate conditions, the occupant preferences, and building parameters (including the efficiencies of wall conduction, window ventilation, and solar radiation from glass). For example, a higher ambient temperature can lead to a faster cooling capacity loss. Currently, first-order equivalent thermal parameter models are widely used to describe the thermal dynamic properties of buildings [11]. Some studies have tapped the peak shaving [12] and frequency regulation [13] capabilities of air conditioners. However, most studies are carried

out based on a fixed COP, which is actually affected by climate conditions significantly.

Above all, this paper focuses on a typical building energy system (BES) integrated PV/T and VESS, as shown in Fig. 1. Considering climate conditions and user satisfaction, an optimal operation model is proposed to accurately assess the energy-saving potential of BES. The main contribution can be summarized as follows:

1) We establish a typical BES model coupling PV/T and VESS, considering varying climate impacts (e.g., solar radiation, ambient temperature, et al) on the conversion efficiency of PV/T, the COP of air conditioners, and the storage capacity of VESS, respectively.

2) An energy-saving potential assessment method is proposed for BES based on the optimal dispatch model for minimizing the electricity consumption, considering the climate impacts and user satisfaction.

The remainder of this paper is organized as follows. Section II presents the BES structure and energy equipment performance model. Section III shows the energy-saving optimal dispatch model. Case study is presented in Section IV. Finally, Section V concludes this paper.

II. ENERGY EQUIPMENT OPERATION MODEL UNDER VARIABLE CLIMATE CONDITIONS

This section proposes a typical BES integrated PV/T, VESS, battery storage and air conditioner, as presented in Fig. 1. The models of each component are developed as follows.

A. Photovoltaic/thermal integrated system

As shown in Fig.1, The PV/T consists of photovoltaic cells, heat collector panels, heat exchanger, heat pump, and heat water tank. The PV/T output is related to dynamic solar radiation and dynamic temperature, as shown in (1)-(5).

$$P_{PV,t} = \eta_{PV,t} I_{solar,t} A_{cell} N_{cell} \quad (1)$$

$$H_{PV,t} = (1 - \alpha - \eta_{PV,t}) I_{solar,t} A_{cell} N_{cell} \quad (2)$$

$$\eta_{PV,t} = \eta_{ref} (1 - \gamma (T_{cell,t} - T_{ref})) \quad (3)$$

$$P_{PV}^{min} \leq P_{PV,t} \leq P_{PV}^{max} \quad (4)$$

$$H_{PV}^{min} \leq H_{PV,t} \leq H_{PV}^{max} \quad (5)$$

where $P_{PV,t}$, $H_{PV,t}$ is the electricity and heat power of PV/T, $\eta_{PV,t}$ is photovoltaic cell efficiency, $I_{solar,t}$ is the solar radiation intensity, A_{cell} is the total cell area, N_{cell} is the total cell number, α is the reflection coefficient, γ is the temperature coefficient, η_{ref} is the reference efficiency of PV module, $T_{cell,t}$ and T_{ref} is the cell temperature and reference temperature.

The heat generated by the PV/T is transferred to the cool water at the heat exchanger. The low-quality hot water is then further heated by the heat pump to high-quality hot water and stored in the heat water tank. The operation constrains of heat pump is shown in (6)-(8).

$$H_{HP,t} = \eta_{HP} P_{HP,t} \quad (6)$$

$$H_{PV,t} + H_{HP,t} = c_p m_{s,t} (T_{s,in,t} - T_{s,out,t}) \quad (7)$$

$$P_{HP}^{max} \leq P_{HP,t} \leq P_{HP}^{min} \quad (8)$$

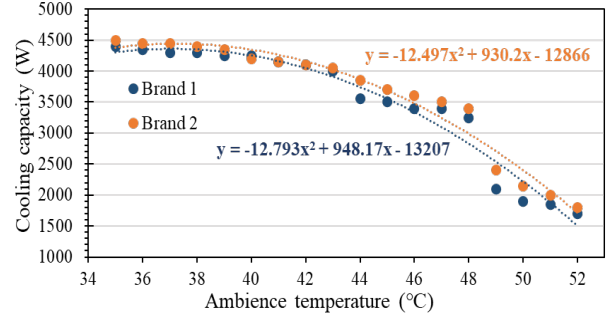


Fig. 2. Experimental data of two brand air conditioners.

where $H_{HP,t}$ and $P_{HP,t}$ are the heat and electricity power of heat pump, c_p is the specific heat capacity of water, $m_{s,t}$ is the water flow, $T_{s,in,t}$ is the inlet water temperature of heat pump, $T_{s,out,t}$ is the outlet water temperature of heat pump, P_{HP}^{max} and P_{HP}^{min} is upper and lower limits of heat pump operation.

B. Air conditioners

Air conditioners consume electrical energy to transfer heat from indoors to outdoors. The refrigeration process of air conditioners includes compression, evaporation, expansion, and condensation, which COP follows the ambient temperature change. We obtained the relationship between the cooling capacity of two different brands of air conditioners and the ambient temperature based on the experimental data, as shown in Fig.2. Further, the relationship between COP and ambient temperature can be fitted as (9). Besides, the operational constrains of air conditioners is shown as (10) (11).

$$COP_{ac,t} = -0.0107T_{a,t}^2 + 0.7901T_{a,t} - 11.0058 \quad (9)$$

$$Q_{ac,t} = COP_{ac,t} P_{ac,t} \quad (10)$$

$$P_{ac}^{min} \leq P_{ac,t} \leq P_{ac}^{max} \quad (11)$$

where $T_{a,t}$ is the ambient temperature, $Q_{ac,t}$ is the cooling power of air conditioner, $P_{ac,t}$ is the electricity power of air conditioner, P_{ac}^{min} and P_{ac}^{max} is upper and lower limits of air conditioner operation.

C. Virtual building energy storage

The building has virtual energy storage capacity due to thermal inertia, which is directly limited by climatic conditions and user satisfaction. The first-order equivalent thermal parameter models are widely used to describe the thermal dynamic properties of buildings, as in (12). The left side represents the indoor temperature change. The right side represents the conductive heat from walls and roofs, convective heat from natural ventilation, solar radiation heat through windows, anthropogenic heat in the room, and cooling from air conditioner. The specific calculation is shown in (13)-(16).

$$\rho c V \frac{dT_{is}}{dt} = Q_{cou,t} + Q_{cov,t} + Q_{rad,t} + Q_{eq,t} - P_{ac,t} \quad (12)$$

$$Q_{cou,t} = (H_w A_w + H_r A_r) (T_{a,t} - T_{is,t}) \quad (13)$$

$$Q_{cov,t} = \rho c q_{is} (T_{a,t} - T_{is,t}) \quad (14)$$

$$Q_{rad,t} = \kappa A_{wo} I_{solar,t} \quad (15)$$

$$Q_{eq,t} = E_{eq} N_f A_r \quad (16)$$

where ρ is the air density, c is the specific heat capacity



Fig.3 The case study in University of Macau.

of air, V is the building volume, $Q_{cou,t}$ is the conductive heat from walls and roofs, $Q_{cov,t}$ is convective heat from natural ventilation, $Q_{rad,t}$ is solar radiation heat through windows, $Q_{eq,t}$ is anthropogenic heat in the room, H_w and H_r is the H value of wall and roof, A_w and A_r is the area of wall and roof, A_{wo} is the area of window, q_{is} is the natural ventilation flow, κ is the radiation efficiency, $E_{eq,t}$ is the indoor anthropogenic heat density, N_f is the number of floor.

III. ENERGY-SAVING OPTIMAL DISPATCH

A. Objection

Based on the structure of BES, the PV/T outputs electricity to meet the demand of uncontrollable loads, air conditioners and heat pumps, while the heat output with heat pumps meets the hot water demand of the building. However, due to the installed capacity limit of PV/T and the uncertainty of power output, BES requires external power purchase to meet the supply-demand balance. To evaluate the energy saving potential of the BES, minimum purchased electricity is used as the optimization objective, as in (17).

$$\min F = \sum_{t \in \varphi_1} P_{grid,t} \quad (17)$$

B. Constraints

1) Energy flow balance

The balance of electricity supply and demand is shown in (18). The left side represents the purchased power, the generation output of PV/T, and the discharge of the battery, respectively. The right side represents the electricity demand of air conditioners, charge of the battery and the uncontrollable load.

$$P_{grid,t} + P_{PV,t} + P_{bs,t}^{dis} = P_{ac,t} + P_{bs,t}^{ch} + P_{L,t} \quad (18)$$

The heat flow balance includes the external circulation balance and the hot water tank balance. In the external circulation, the low-quality hot water from the hot water tank is heated by the heat exchanger and heat pump, with the constant water flow rate $m_{s,t}$. Meanwhile the heat flow balance has shown in (7). In the hot water tank balance, the total amount of water and mixed heat flow are constant, as shown in (19).

$$c_p m_{s,t} T_{s,in,t} + c_p m_{l,t} T_{l,in,t} = c_p m_{s,t} T_{s,out,t} + c_p m_{l,t} T_{l,out,t} \quad (19)$$

where $m_{l,t}$ is the load water flow, $T_{l,in,t}$ is the temperature

of cool water source, $T_{l,out,t}$ is the temperature of hot water load.

2) Battery

The operational constraints of the battery include state of charge (20), capacity (21) (22), charging and discharging power (23) (24), and operational status (25) [14].

$$E_{bs,t} = (1 - \varepsilon) E_{bs,t-1} + \lambda_{bs}^{ch} P_{bs,t}^{ch} - \left(\frac{1}{\lambda_{bs}^{dis}} \right) P_{bs,t}^{dis} \quad (20)$$

$$E_{bs}^{\min} \leq E_{bs,t} \leq E_{bs}^{\max} \quad (21)$$

$$E_{bs,0} = E_{bs,T} \quad (22)$$

$$0 \leq P_{bs,t}^{ch} \leq A(t) P_{bs}^{ch,max} \quad (23)$$

$$0 \leq P_{bs,t}^{dis} \leq B(t) P_{bs}^{dis,max} \quad (24)$$

$$A(t) + B(t) \leq 1 \quad (25)$$

where $E_{bs,t}$ is the state of charge (SOC) of battery, ε is energy loss rate, λ_{bs}^{ch} and λ_{bs}^{dis} is the charge/discharge efficiency, E_{bs}^{\min} and E_{bs}^{\max} is the lower and upper limit of SOC, $P_{bs,t}^{ch}$ and $P_{bs,t}^{dis}$ is the charge/discharge power, $A(t)$ and $B(t)$ is the state functions of charge and discharge.

IV. CASE STUDY

A. Test system

The proposed model was tested in 59 buildings of the University of Macau as shown in Fig.3, with an effective floor area of 243,439.63 m². Three comparison scenarios are used to analyze the energy saving potential of the buildings: Case 1 is the current basic scenario without considering PV/T and VESS, Case 2 is optimal scenario considering VESS and user satisfaction, Case 3 is the future scenario that building is equipped with PV/T on the roof. The parameters are setting as shown in Tab.1 and the area of PV/T cell equals to the roof in Case 3.

Tab.1 The parameters setting [9].

	Values		Values
η_{PV}	0.3	ρ	1.225 kg/m ³
α	0.2	c	1030 J/(kg·K)
γ	0.0045	H_w	0.4 W/(m ² ·K)
η_{ref}	0.12	H_r	0.2 W/(m ² ·K)
T_{ref}	298 K	q_{is}	1.0 m ³ /h
η_{HP}	0.9	E_{eq}	19 W/m ²
c_p	4200 J/(kg·K)	ε	0.1

B. Energy-saving potential

Fig.4 shows the COP curve of air conditioners considering the ambient climate conditions. It can be found that as the temperature of the operating environment increases, the cooling capacity of the air conditioner decreases. Between 12:00 and 14:00 at noon, the COP decreases to below 2.5, which means that 30% of the electricity is consumed additionally. Therefore, when the ambient temperature rises, conduction, convection and radiation heat will increase the indoor cooling load demand. Meanwhile, the COP of the air conditioner will decrease, which will lead to a spike in electricity consumption, as shown in Fig.5 Case1.

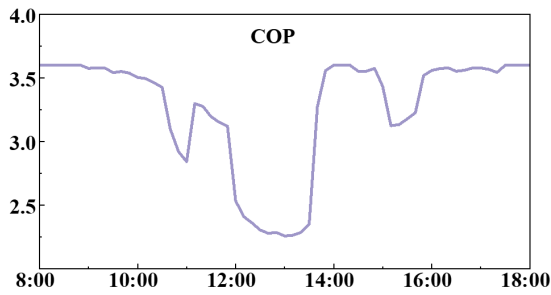


Fig.4 The COP of air conditioner considering the operational climate condition

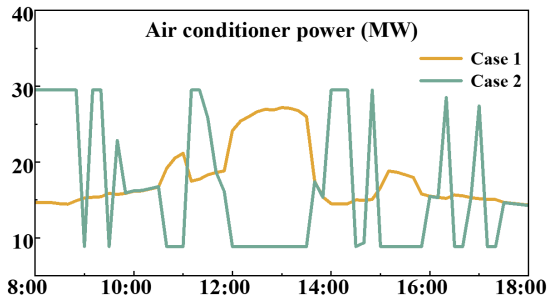


Fig.5 The electricity power consumption of air conditioner

In Case2, the virtual energy storage capacity of the building is tapped to store the cooling capacity while meeting the comfort requirements of the occupants. As in Case2 of Fig. 5 and Fig.6, the building virtual energy storage supports the air conditioner to increase the extra output during the periods with high COP while ensuring that the indoor temperature is maintained within the comfort zone, such as the hours 11:00-12:00. Then, the cooling volume stored in the building keeps the room cooler during the hours with reduced COP, which improves the efficiency of power utilization.

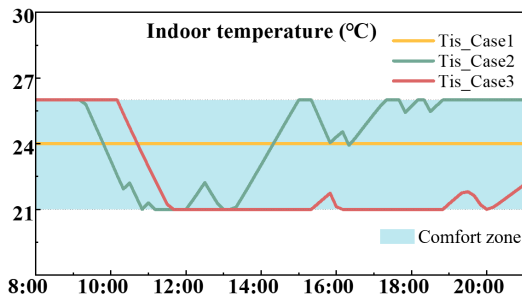


Fig.6 The indoor temperature change considering the user satisfaction.

PV/T is an efficient pathway for renewable energy utilization, outputting electricity while meeting the building heat load. During peak periods of solar radiation, PV/T installed on the roof can meet the indoor hot water load, while the excess power is stored in the battery, as shown in Fig. 7 and Fig.8. At the same time, the air conditioner cooperates with the building virtual energy storage to realize the consumption of excess PV and further enhance the energy utilization efficiency. After the sun goes down, the electricity stored in the batteries is released to meet the heat load demand in conjunction with the heat pump.

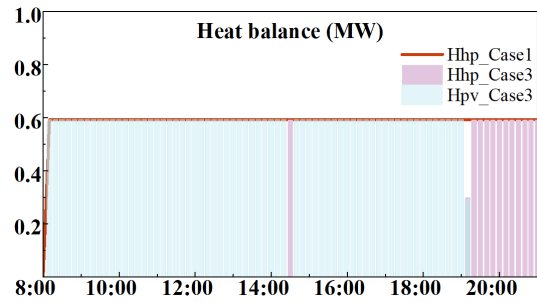


Fig.7 The heat output of heat pump and PV/T

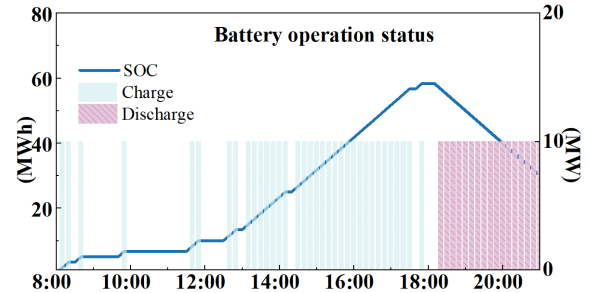


Fig.8 Battery operation status in Case 3

Fig. 9 shows the energy saving potential of the University of Macau buildings in Case 1-3. Based on the building virtual energy storage, the purchased electricity of the building energy system can be reduced by 15%. Furthermore, in the future scenario, all building rooftops are equipped with PV/T. At this point, considering the cooperative optimization of virtual energy storage and PV/T, the purchased electricity of the building energy system can be reduced by 76%. In particular, the main loads of the building are satisfied by renewable energy sources, which promotes zero carbon emissions on campus.

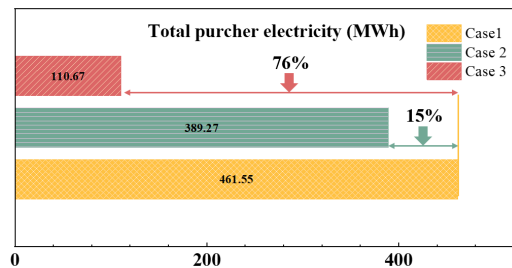


Fig.9 The energy-saving potential of BES considering VESS and PV/T.

V. CONCLUSION

An energy-saving potential assessment model is proposed in this paper considering climate impacts. Numerical relationships between varying climate conditions (solar radiation, temperature) and PV/T conversion efficiency, coefficient of performance (COP) for air conditioners, and storage capacity of VESS are developed, respectively. Simulation results on building block in University of Macau demonstrate that the building virtual energy storage can achieve 15% energy savings. Meanwhile, the cooperation between PV/T and building virtual energy storage is a promising way for zero carbon emissions, which can achieve 76% energy savings.

REFERENCES

- [1] IEA. Global Status Report for Buildings and Construction 2019[R]. Paris: IEA, 2019.
- [2] Huang B, Huang S, Ma X, et al. Stochastic scheduling for commercial building cooling systems: considering uncertainty in zone temperature prediction[J]. *Applied Energy*, 2023, 346: 121367.
- [3] Han Y, Ma L, Zhang J, et al. Research on the adaptive proportional-integral control method of a direct-expansion photovoltaic-thermal heat pump system[J]. *Energy*, 2023: 128077.
- [4] Yao W, Wang C, Yang M, et al. A tri-layer decision-making framework for IES considering the interaction of integrated demand response and multi-energy market clearing[J]. *Applied Energy*, 2023, 342: 121196.
- [5] Zhang Z, Wang C, Chen S, et al. Multitime scale co-optimized dispatch for integrated electricity and natural gas system considering bidirectional interactions and renewable uncertainties[J]. *IEEE Transactions on Industry Applications*, 2022, 58(4): 5317-5327.
- [6] Khanegah M R, Ashrafizadeh A, Borooghani D, et al. Performance Evaluation of a Concentrated Photovoltaic/thermal System based on Water and Phase Change Material: Numerical Study and Experimental Validation[J]. *Applied Thermal Engineering*, 2023: 120936.
- [7] Lu Shixiang, Liang Ruobing, Zhang Jili, et al. Performance improvement of solar photovoltaic/ thermal heat pump system in winter by employing vapor injection cycle[J]. *Applied Thermal Engineering*, 2019, 155:135-146.
- [8] Ding Y, Xie D, Hui H, et al. Game-theoretic demand side management of thermostatically controlled loads for smoothing tie-line power of microgrids[J]. *IEEE Transactions on Power Systems*, 2021, 36(5): 4089-4101.
- [9] Hui H, Ding Y, Liu W, et al. Operating reserve evaluation of aggregated air conditioners[J]. *Applied energy*, 2017, 196: 218-228.
- [10] Mu Y, Xu Y, Zhang J, et al. A data-driven rolling optimization control approach for building energy systems that integrate virtual energy storage systems[J]. *Applied Energy*, 2023, 346: 121362.
- [11] Zhuang C, Choudhary R, Mavrogianni A. Uncertainty-based optimal energy retrofit methodology for building heat electrification with enhanced energy flexibility and climate adaptability[J]. *Applied Energy*, 2023, 341: 121111.
- [12] Hui H, Siano P, Ding Y, et al. A transactive energy framework for inverter-based HVAC loads in a real-time local electricity market considering distributed energy resources[J]. *IEEE Transactions on Industrial Informatics*, 2022, 18(12): 8409-8421.
- [13] Chen G, Zhang H, Hui H, et al. Fast Wasserstein-distance-based distributionally robust chance-constrained power dispatch for multi-zone HVAC systems[J]. *IEEE Transactions on Smart Grid*, 2021, 12(5): 4016-4028.
- [14] Zhang Z, Wang C, Lv H, et al. Day-ahead optimal dispatch for integrated energy system considering power-to-gas and dynamic pipeline networks[J]. *IEEE Transactions on Industry Applications*, 2021, 57(4): 3317-3328.